

Long-range donor-acceptor electron transport mediated by α -helices

L.S. Brizhik*,

Bogolyubov Institute for Theoretical Physics, 03143 Kyiv, Ukraine

Jingxi Luo[†]

School of Mathematics, University of Birmingham,
Birmingham B15 2TT, UK

B.M.A.G. Piette[‡] and W.J. Zakrzewski[§]

Department of Mathematical Sciences, University of Durham,
Durham DH1 3LE, UK

Abstract

We study the long-range electron and energy transfer mediated by a polaron on an α -helix polypeptide chain coupled to donor and acceptor molecules at opposite ends of the chain. We show that for specific parameters of the system, an electron initially located on the donor can tunnel onto the α -helix, forming a polaron which then travels to the other extremity of the polypeptide chain where it is captured by the acceptor. We consider three families of couplings between the donor, acceptor and the chain, and show that one of them can lead to a 90% efficiency of the electron transport from donor to acceptor. We also show that this process remains stable at physiological temperatures in the presence of thermal fluctuations in the system.

PACS numbers: 05.45.Yv, 05.60.-k, 63.20.kd, 71.38.-k

Key words: long-range donor-acceptor electron and energy transfer, large polaron, alpha-helix, donor-bridge-acceptor complex, soliton, self-trapping

*e-mail address: brizhik@bitp.kiev.ua

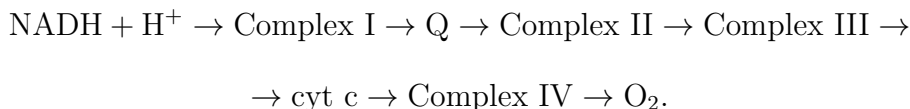
[†]e-mail address: j.luo.5@bham.ac.uk

[‡]e-mail address: B.M.A.G.Piette@durham.ac.uk

[§]e-mail address: w.j.zakrzewski@durham.ac.uk

1 Introduction

The mechanisms behind the highly efficient long-range electron transfer (ET) in redox reactions accompanying photosynthesis and cellular respiration have been intensively discussed over several decades [1, 2]. This transfer takes place at macroscopic distances along the so-called electron transport chain in Krebs cycles in membranes of chloroplasts, mitochondria or cells, and occurs at physiological temperatures. Conventional mechanisms, such as tunnelling, Forster and Dexter mechanism etc. [3, 4, 5], cannot provide such long-range ET even at zero temperature, let alone 300 K. Nevertheless, it should be noticed that the very structure of the ET chain can facilitate these processes. An ET chain consists of a spatially separated sequence of biological molecular complexes (peptides, enzymes, etc.), along which the sequential transport of electrons takes place via the redox processes, so that every site in this chain plays the role of an acceptor for the left neighbour and donor for the right one along the chain (see, e.g., [6]). The electron transport chain in mitochondria can be schematically represented as the following sequence:



Here $\text{NADH} + \text{H}^+$ is nicotinamide adenine dinucleotide, which serves as the substrate; Complex I is NADH coenzyme Q reductase; Q is ubiquinone coenzyme; Complex II is succinate dehydrogenase; Complex III is cytochrome bc_1 ; cyt c is cytochrome c ; Complex IV is cytochrome c oxidase; O_2 is molecular oxygen.

In each elementary process, at the initial moment, there is a release of four electrons at the substrate, which then are carried along the chain with the reduction of molecular oxygen and hydrogen ions to a water molecule at the final stage of the process. This transport of electrons is so exceptionally efficient that only a tiny percentage of electrons leak out to reduce oxygen, directly generating superoxide which results in oxidative stress and leads to various diseases. The complexes in the ET chain can be conventionally divided into two groups: heavy and light ones. In particular, in ET chains, such elements as ubiquinone or cytochrome $cyt-c$, have relatively small molecular weight which leads to their high solubility. They can move outside the mitochondrial membrane, carrying electrons from a heavy donor to a heavy acceptor via a linear, *e.g.* Forster, mechanism [3, 5]. Some other complexes in the electron transport chain, such as NADH-ubiquinone oxidoreductase, flavoproteins, cytochrome c -oxidase, cyt aa_3 and cytochrome $cyt bc_1$ complexes

are proteins with large molecular weight of up to several hundreds of kiloDaltons. Conventional linear mechanisms cannot provide coherent transport of electrons across these heavy enzymes. Nevertheless, their regular crystal-like structure can facilitate ET, as is discussed below.

A significant part of heavy macromolecules is in the alpha-helical conformation, whose regular structure results in the formation of electron bands in their energy spectrum. The alpha-helical structure is stabilized by relatively weak hydrogen bonds resulting in strong electron-lattice interactions, and thus, in the polaron effect. An α -helical segment of a protein contains three almost-parallel polypeptide strands bound by hydrogen bonds along the strands, with weak interactions between these strands. An isolated strand is described by the Fröhlich Hamiltonian, and this description leads to a system of coupled nonlinear equations for the electron wavefunction and lattice variables, and admits soliton solutions. The possibility of self-trapping of electrons in an isolated one-dimensional molecular chain, like a polypeptide strand, has been first shown in [7] (see also [8, 9]) and later it was also demonstrated in helical systems [10, 11, 12]. The soliton solutions of these models are particular cases of a large polaron. It can be described as a crossover between an almost-free electron and small polaron states depending on the strength of the exchange interaction energy, electron-lattice coupling constant, the number of phonon modes, their type and the corresponding Debye energies [13]. The soliton properties depend on the parameters of the system. Moreover, the helical structure of proteins was shown to lead to the existence of several types of soliton solutions of the model with different properties and symmetries [12]. In such soliton states electrons can propagate along macromolecules almost without any loss of energy.

The results mentioned above have been obtained for isolated strands or helices, while in reality, the electron transport occurs in the system Donor-Bridge-Acceptor, as is the case of the ET chain in the Krebs cycles. The simple case when the bridge is modelled as a polypeptide strand had been studied in [14]. It was shown there that the long-range ET can be provided by the soliton mechanism within a wide range of parameter values of donor, acceptor and polypeptide strands.

In the present paper we study the possibility of a coherent long-range electron transport in the system Donor- α -helix-Acceptor. As one can expect, the formation of the soliton on the α -helix depends on the initial conditions of the electron tunnelling to the boundary of the helix, as well as on the parameters of the system under study (see *e.g.*, [14, 15, 16]), and we can find conditions which lead to the formation of a soliton on the helix.

There are two other aspects of the model developed in the present paper. The first one is related to the fact that the functioning of the ET chain

is tightly connected with the production of adenosine triphosphate (ATP) whose hydrolysis is the main source of biological energy: in most organisms the majority of ATP is generated in ET chains (see, *e.g.*, [17]). It is well known that the energy released in the hydrolysis of ATP is stored in the form of the Amide-I vibration, which can be self-trapped into a soliton state and carried along the associated macromolecules to the place where it is utilized for biochemical or mechanical needs [8, 9]. This process, from the mathematical point of view, is described by formally the same system of equations as the ET. Therefore, the results obtained here are equally valid for such energy transfer processes.

The second aspect of the model is related to the potential importance of our results for micro- and nano-electronics where conjugated donor-acceptor copolymer semiconductors with intra-molecular charge transfer on large distances are widely used. A large number of such systems have been recently synthesized. They include donor-acceptor pairs mediated by salt bridges [18], thienopyrazine-based copolymers [19] and some others [20, 21, 22]. Donor-bridge-acceptor systems with efficient ET play an important role in electronic applications [23, 24, 25, 26]: they can be used in photovoltaic cells [27, 28, 29, 22], light-emitting diodes [30, 31, 32, 33] and field-effect transistors [34, 35, 36, 37], in particular, thin-film organic field effect transistors [38]. Proteins and synthetic macromolecules and a great technological potential; one example is the improvement of efficiency and UV-photostability of planar perovskite solar cells using amino-functionalized conjugated polymers as ET materials [20, 22]. This is one of the facts which have stimulated our interest in the problems discussed in the present paper.

In the first section of the paper we derive a model of the α -helix coupled to a donor molecule and an acceptor molecule. This is a combination of the models derived in [12] and [14]. We then perform a parameter scaling to make all the parameters dimensionless and derive the equations in such units. After selecting the parameters that best describe the α -helical protein, we compute the profile of a static self-trapped electron state (soliton-like or, in other words, large polaron state, which for simplicity we call from now on a ‘polaron’) by solving the model equations numerically. We then study various configurations where the electron density has been set to 1 on the donor and 0 elsewhere and let the system evolve. We do this for three different types of couplings between the donor and acceptor to the α -helix and we determine numerically the donor and acceptor coupling parameters that lead to the best transfers of the electron. We end the paper by describing the solutions we have found and draw some conclusions.

2 Model of the System ‘Donor – α -Helix – Acceptor’

We consider a polypeptide chain in an α -helical configuration made out of N peptides, with a donor molecule attached to one end and an acceptor molecule attached to the other end. The peptide chain forms a helical structure in which each molecule is coupled by chemical bonds to its neighbours along the chain as well as to the molecules 3 sites away from it by hydrogen bonds. With this 3-step coupling, the α -helix can also be seen as 3 parallel chains [39] which we refer to as strands in what follows. This model is depicted in figure 1.

We label the molecules with the index n along the polypeptide chain, and use $n = 0$ for the donor and $n = N + 1$ for the acceptor. This means that peptides with an index difference which is a multiple of 3 belong to the same strand of the α -helix.

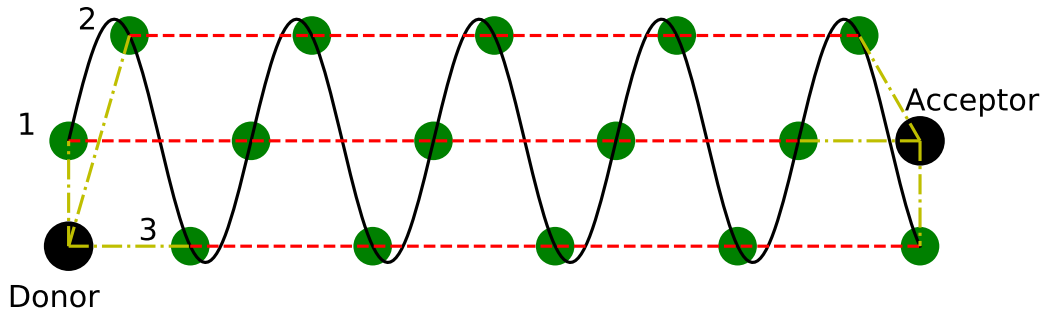


Figure 1: The model of α -helix with a donor and an acceptor. The continuous lines represent the links along the polypeptide chain, the dash lines represent the links along the strands and the dash-dot lines the links between the donor/acceptor and the different strands. The numbers 1, 2 and 3 label the 3 strands.

The donor and the acceptor can, *a-priori*, be coupled respectively to the first 3 or the last 3 peptides, *i.e.*, with the nodes $n = 1, 2, 3$ and $N = N - 2, N - 1, N$. In our study, we will consider 3 different types of couplings but for now, we assume that all the coupling parameters are different.

The Hamiltonian of the system is given by

$$\mathcal{H} = \mathcal{H}_p + \mathcal{H}_e + \mathcal{H}_{int}, \quad (1)$$

where

$$\begin{aligned}
\mathcal{H}_e &= \bar{\mathcal{E}}_d |\Psi_0|^2 + \bar{\mathcal{E}}_a |\Psi_{N+1}|^2 + \bar{\mathcal{E}}_0 \sum_{n=1}^N |\Psi_n|^2 - \bar{J} \sum_{n=1}^{N-3} \left(\Psi_n \Psi_{n+3}^* + \Psi_{n+3} \Psi_n^* \right) \\
&+ \bar{L} \sum_{n=1}^{N-1} \left(\Psi_n \Psi_{n+1}^* + \Psi_{n+1} \Psi_n^* \right) - \sum_{\ell=1}^3 \bar{D}_{d,\ell} (\Psi_0 \Psi_\ell^* + \Psi_\ell \Psi_0^*) \\
&- \sum_{\ell=1}^3 \bar{D}_{a,\ell} (\Psi_{N+1} \Psi_{N-3+\ell}^* + \Psi_{N-3+\ell} \Psi_{N+1}^*), \tag{2}
\end{aligned}$$

$$\begin{aligned}
\mathcal{H}_p &= \frac{1}{2} \left[\frac{P_d^2}{M_d} + \frac{P_a^2}{M_a} \right] + \frac{1}{2} \sum_{\ell=1}^3 \left[\bar{W}_{d,\ell} (U_0 - U_\ell)^2 + \bar{W}_{a,\ell} (U_{N+1} - U_{N-3+\ell})^2 \right] \\
&+ \frac{1}{2} \sum_{n=1}^N \frac{P_n^2}{M} + \frac{1}{2} \sum_{n=1}^{N-3} \bar{W} (U_{n+3} - U_n)^2, \tag{3}
\end{aligned}$$

$$\begin{aligned}
\mathcal{H}_{int} &= |\Psi_0|^2 \sum_{\ell=1}^3 \bar{\chi}_{d,\ell} (U_\ell - U_0) + |\Psi_{N+1}|^2 \sum_{\ell=1}^3 \bar{\chi}_{a,\ell} (U_{N+1} - U_{N-3+\ell}) \\
&+ \sum_{\ell=1}^3 |\Psi_\ell|^2 \left[\bar{\chi}_{d,\ell} (U_\ell - U_0) + \bar{\chi} (U_{\ell+3} - U_\ell) \right] \\
&+ \sum_{\ell=1}^3 |\Psi_{N-3+\ell}|^2 \left[\bar{\chi}_{a,\ell} (U_{N+1} - U_{N-3+\ell}) + \bar{\chi} (U_{N-3+\ell} - U_{N-6+\ell}) \right] \\
&+ \bar{\chi} \sum_{n=4}^{N-3} |\Psi_n|^2 (U_{n+3} - U_{n-3}). \tag{4}
\end{aligned}$$

In these expressions, $\bar{\mathcal{E}}_0$ describes the on-site electron energy, \bar{J} the resonance integral along the strands, \bar{L} the resonance integral along the helix, M the mass of the unit cell, $\bar{\chi}$ the electron-lattice coupling and \bar{W} the elasticity of the bond along the strands. The constants with subscript d and a refer to parameters of the donor and the acceptor respectively.

The functions Ψ_n describe the electron wave function (and so $|\Psi_n|^2$ describe the electron probability of being at the site n) and U_n describe the displacement of molecule n along the strands. P_n are the canonically conjugated momenta of U_n . Of course, the electron wave function satisfies the normalization condition

$$\sum_{n=0}^{N+1} |\Psi_n|^2 = 1, \tag{5}$$

where, following our convention, $\Psi_0 = \Psi_d$ and $\Psi_{N+1} = \Psi_a$.

Our model is meant to describe the case in which the principal chain can be sufficiently well approximated by one electron band and one acoustical phonon mode which describes the longitudinal displacements of the unit cells from their positions of equilibrium along the helix's strands. The electron-lattice interaction Hamiltonian induces a dependence of the electron Hamiltonian on the lattice distortions. We also assume here that the dependence of the on-site electron energy on the lattice distortion is much weaker than that of the inter-site electron interaction energy.

The model we present here is a combination of the polaron model of the α -helix which was described in detail in [12] and of the donor-acceptor model described in [14]. The first model describes polarons on an α -helix, instead of using the traditional single chain, proposed by Davydov [8, 9], which corresponds to what we call a strand in this paper. In fact, it was shown in [12] that the polaron is spread over the 3 strands hence the relevance of using a more realistic helical model. The second paper describes a model of the spontaneous transfer of an electron from a donor molecule to an acceptor one via the propagation of a polaron along a simple chain (a single strand in the present model). The model we describe here is a combination of these two models in which the donor and the acceptor are coupled to a proper α -helix instead of a single strand.

3 Parameter scaling

To facilitate the analysis of the model solutions, it is convenient to scale the parameters so that they become dimensionless. Thus, following [12], we perform the following scalings:

$$\begin{aligned}
d &= 10^{-11} \text{ m}, & u_n &= \frac{U_n}{d}, & \tau &= t\nu, \\
\mathcal{E}_0 &= \frac{\bar{\mathcal{E}}_0}{\hbar\nu}, & \mathcal{E}_d &= \frac{\bar{\mathcal{E}}_d}{\hbar\nu}, & \mathcal{E}_a &= \frac{\bar{\mathcal{E}}_a}{\hbar\nu}, \\
J &= \frac{J}{\hbar\nu}, & D_a &= \frac{D_a}{\hbar\nu}, & L &= \frac{L}{\hbar\nu}, & D_d &= \frac{\bar{D}_a}{\hbar\nu}, \\
W &= \frac{\bar{W}}{\nu^2 M}, & W_{d,\ell} &= \frac{\bar{W}_{d,\ell}}{\nu^2 M}, & W_{a,\ell} &= \frac{\bar{W}_{a,\ell}}{\nu^2 M}, \\
\chi &= \frac{d\bar{\chi}}{\hbar\nu}, & \chi_{d,\ell} &= \frac{d\bar{\chi}_{d,\ell}}{\hbar\nu}, & \chi_{a,\ell} &= \frac{d\bar{\chi}_{a,\ell}}{\hbar\nu}, \\
K_d &= \frac{M}{M_d}, & K_a &= \frac{M}{M_a}, & G &= \frac{\hbar}{d^2 M \nu}.
\end{aligned} \tag{6}$$

As a result, the Hamiltonian becomes $\mathcal{H}_p = M \nu^2 d^2 H_p$, $\mathcal{H}_e = \hbar \nu H_e$ and $\mathcal{H}_{int} = \hbar \nu H_{int}$ where

$$H_e = \mathcal{E}_d |\Psi_0|^2 + \mathcal{E}_a |\Psi_{N+1}|^2 + \mathcal{E}_0 \sum_{n=1}^N |\Psi_n|^2 - J \sum_{n=1}^{N-3} \left(\Psi_n \Psi_{n+3}^* + \Psi_{n+3} \Psi_n^* \right)$$

$$\begin{aligned}
& + L \sum_{n=1}^{N-1} \left(\Psi_n \Psi_{n+1}^* + \Psi_{n+1} \Psi_n^* \right) - \sum_{\ell=1}^3 D_{d,\ell} (\Psi_0 \Psi_\ell^* + \Psi_\ell \Psi_0^*) \\
& - \sum_{\ell=1}^3 D_{a,\ell} (\Psi_{N+1} \Psi_{N-3+\ell}^* + \Psi_{N-3+\ell} \Psi_{N+1}^*), \tag{7}
\end{aligned}$$

$$\begin{aligned}
H_p = & \frac{1}{2} \left[\frac{1}{K_d} \left(\frac{du_0}{dt} \right)^2 + \frac{1}{K_a} \left(\frac{du_{N+1}}{dt} \right)^2 \right] + \\
& + \frac{1}{2} \sum_{\ell=1}^3 \left[W_{d,\ell} (u_0 - u_\ell)^2 + W_{a,\ell} (u_{N+1} - u_{N-3+\ell})^2 \right] \\
& + \frac{1}{2} \sum_{n=1}^N \left(\frac{du_n}{dt} \right)^2 + \frac{1}{2} \sum_{n=1}^{N-3} W (u_{n+3} - u_n)^2, \tag{8}
\end{aligned}$$

$$\begin{aligned}
H_{int} = & |\Psi_0|^2 \sum_{\ell=1}^3 \chi_{d,\ell} (U_\ell - U_0) + |\Psi_{N+1}|^2 \sum_{\ell=1}^3 \chi_{a,\ell} (U_{N+1} - U_{N-3+\ell}) \\
& + \sum_{\ell=1}^3 |\Psi_\ell|^2 [\chi_{d,\ell} (U_\ell - U_0) + \chi (U_{\ell+3} - U_\ell)] \\
& + \sum_{\ell=1}^3 |\Psi_{N-3+\ell}|^2 [\chi_{a,\ell} (U_{N+1} - U_{N-3+\ell}) + \chi (U_{N-3+\ell} - U_{N-6+\ell})] \\
& + \chi \sum_{n=4}^{N-3} |\Psi_n|^2 (U_{n+3} - U_{n-3}). \tag{9}
\end{aligned}$$

We must thus have $M \nu^2 d^2 = \hbar \nu$ and so $\nu = \hbar / (M d^2)$. With $M = 1.9112 \cdot 10^{-25}$ kg [14] and, as $\hbar = 1.054 \cdot 10^{-34}$ Js, we have $\nu = 5.51 \times 10^{12}$ s⁻¹. Moreover, this also implies that $G = 1$.

Before deriving the dimensionless equations it is also convenient to multiply the wave function by a time-dependent phase and so we define

$$\psi(t) = \Psi(t) \exp \left(-\frac{it}{\hbar} (\bar{\mathcal{E}}_0 + 2\bar{L} - 2\bar{J}) \right). \tag{10}$$

Following [14] we also need to add a tunnelling term of the form $i \sum_{\ell=1}^3 A_{a,\ell} |\psi_{N-3+\ell}|^2 \psi_{N+1}$ to the electron equation for the acceptor. This extra term has the properties that it induces the capture of the electron by the acceptor while conserving the total electron probability.

From the above Hamiltonian (1,7,8,9) one can easily derive the following

equations for U_n and Ψ_n :

$$\begin{aligned}
i\frac{d\Psi_0}{d\tau} &= (\mathcal{E}_d - \mathcal{E}_0 - 2L + 2J)\Psi_0 - \sum_{\ell=1}^3 D_{d,\ell}\Psi_\ell + \Psi_0 \sum_{\ell=1}^3 \chi_{d,\ell}(u_\ell - u_0) \\
i\frac{d\Psi_\ell}{d\tau} &= (2J - 2L)\Psi_\ell - J\Psi_{\ell+3} + L(\Psi_{\ell+1} + \Psi_{\ell-1}(1 - \delta_{\ell,1})) - D_{d,\ell}\Psi_0 \\
&\quad + \chi_{d,\ell}\Psi_\ell(u_\ell - u_0) + \chi\Psi_\ell(u_{\ell+3} - u_\ell), \quad \ell = 1, 2, 3 \\
i\frac{d\Psi_n}{d\tau} &= (2J - 2L)\Psi_n - J(\Psi_{n+3} + \Psi_{n-3}) + L(\Psi_{n+1} + \Psi_{n-1}) + \chi\Psi_n(u_{n+3} - u_{n-3}), \\
&\quad n = 4 \dots N - 3 \\
i\frac{d\Psi_{N-3+\ell}}{d\tau} &= (2J - 2L)\Psi_{N-3+\ell} - J\Psi_{N-6+\ell} + L(\Psi_{N-4+\ell} + \Psi_{N-2+\ell}(1 - \delta_{\ell,3})) - D_{a,\ell}\Psi_{N+1} \\
&\quad + \chi_{a,\ell}\Psi_{N-3+\ell}(u_{N+1} - u_{N-3+\ell}) + \chi\Psi_{N-3+\ell}(u_{N-3+\ell} - u_{N-6+\ell}), \\
&\quad -iA_{a,\ell}|\Psi_{N+1}|^2\Psi_{N-3+\ell} \quad \ell = 1, 2, 3 \\
i\frac{d\Psi_{N+1}}{d\tau} &= (\mathcal{E}_a - \mathcal{E}_0 + 2J - 2L)\Psi_{N+1} - \sum_{\ell=1}^3 D_{a,\ell}\Psi_{N-3+\ell} + \Psi_{N+1} \sum_{\ell=1}^3 \chi_{a,\ell}(u_{N+1} - u_{N-3+\ell}) \\
&\quad + i\sum_{\ell=1}^3 A_{a,\ell}|\Psi_{N-3+\ell}|^2\Psi_{N+1} \\
\frac{d^2u_0}{d\tau^2} &= K_d\left(\sum_{\ell=1}^3 W_{d,\ell}(u_\ell - u_0) + \sum_{\ell=1}^3 \chi_{d,\ell}(|\Psi_0|^2 + |\Psi_\ell|^2)\right) \\
\frac{d^2u_\ell}{d\tau^2} &= W(u_{\ell+3} - u_\ell) + W_{d,\ell}(u_0 - u_\ell) - \chi_{d,\ell}(|\Psi_0|^2 + |\Psi_\ell|^2) + \chi(|\Psi_\ell|^2 + |\Psi_{\ell+3}|^2) \\
&\quad \ell = 1, 2, 3 \\
\frac{d^2u_n}{d\tau^2} &= W(u_{n+3} + u_{n-3} - 2u_n) + \chi(|\Psi_{n+3}|^2 - |\Psi_{n-3}|^2) \quad n = 4 \dots N - 3 \\
\frac{d^2u_{N-3+\ell}}{d\tau^2} &= W(u_{N-6+\ell} - u_{N-3+\ell}) + W_{a,\ell}(u_{N+1} - u_{N-3+\ell}) \\
&\quad + \chi_{a,\ell}(|\Psi_{N+1}|^2 + |\Psi_{N-3+\ell}|^2) - \chi(|\Psi_{N-3+\ell}|^2 + |\Psi_{N-6+\ell}|^2) \quad \ell = 1, 2, 3 \\
\frac{d^2u_{N+1}}{d\tau^2} &= K_a\left(\sum_{\ell=1}^3 W_{a,\ell}(u_{N-3+\ell} - u_{N+1}) - \sum_{\ell=1}^3 \chi_{a,\ell}(|\Psi_{N+1}|^2 + |\Psi_{N-3+\ell}|^2)\right) \quad (11)
\end{aligned}$$

where $\delta_{i,j}$ is the Kronecker delta function. We now need to select the parameter values that best describe the α -helix.

3.1 Parameter values

For the numerical modelling we need to use some numerical values of the parameters. We recall that, in particular, the parameter values for the

polypeptide macromolecules are: $J_{\text{Amide-I}} = 1.55 \cdot 10^{-22}$ Joules $\approx 10^{-3}$ eV; $J_e \approx 0.1 - 0.01$ eV $\approx 10^{-21} - 10^{-20}$ Joules; $\chi = (35 - 62)$ pN; $w = 39 - 58$ N/m, $V_{ac} = (3.6 - 4.5) \cdot 10^3$ m/s [9]. Molecular weights of large macromolecules which participate in the electron transport chain in redox processes are: NADH-ubiquinone oxidoreductase - 980 kDa; cytochrome bc_1 complex - 480 kDa; cytochrome $c - aa_3$ oxidase - 420 kDa. Mass of Cyt-c is 12 kDa, in which the hem-A group has a molecular weight 852 Da, and hem-B group has 616 Da, which are 3-5 times larger than the molecular weight 100-200 Da of amino-acids that form macromolecules. Study of the of the mitochondrial ET chain shows that electrochemical potential for the transfer of the electrons is $E_{e-c} = +1.135$ V [41, 42].

For completeness of the study we also summarize the data on the parameter values of other relevant compounds in accordance with the discussion in Introduction. Molecular weights of many conjugated polymer semiconductors vary in the interval (10 - 176) kDa, and the hole mobility is $4 \cdot 10^{-4} - 1.6 \cdot 10^{-3}$ $\text{cm}^2 / (\text{V s})$. Ionization potential and electron affinity potential for some donor-acceptor copolymer semiconductor molecules are: (2.5-4.5) eV and (1.5-3.1) eV, respectively [43]. The electrochemical band gap is $E_g^{(el)} = E_{IP} - E_{EA}$ is 1.5 eV for BTTP, 1.84 eV for BTTP-P, and 2.24 eV for BTTP-F, which are 0.4-0.6 eV larger from the optically determined ones $E_g^{(opt)} = 1.1 - 1.6$ eV. This difference can be explained by the exciton binding energy of conjugated polymers which is thought to be in the range of $E_{ex} \approx 0.4 - 1.0$ eV [44]. Thieno pyrazine-based donor-acceptor copolymers, such as BTTP, BTTP-T, BTTP-F, BTTP-P, have moderate to high molecular weights, broad optical absorption bands that extend into the near-infrared region with absorption maxima at 667-810 nm, and small optical band gaps (1.1 - 1.6 eV). They show ambipolar redox properties with low ionization potentials (HOMO levels) of (4.6-5.04) eV. The field-effect mobility of holes varies from $4.2 \cdot 10^{-4}$ $\text{cm}^2 / (\text{V s})$ in BTTP-T to $1.6 \cdot 10^{-3}$ $\text{cm}^2 / (\text{V s})$ in BTTP-F (see [19]). The reduction potentials of BTTP, BTTP-P, and BTTP-F are -1.4, -1.73, and -1.9 V (vs SCE), respectively. The oxidation potentials of the copolymers are in the range 0.29- 0.71 V (vs SCE). The onset oxidation potential and onset reduction potential of the parent copolymer BTTP are 0.2 and -1.3 V, respectively, which give an estimate for the ionization potential (IP, HOMO level) of 4.6 eV ($E_{IP} = E_{ox}^{onset} + 4.4$) and an electron affinity (EA, LUMO level) of 3.1 eV ($E_{EA} = E_{red}^{onset} + 4.4$). The 4.6 eV E_{IP} value of BTTP is 0.3 eV less than that of poly(3- hexylthiophene) (4.9 eV), whereas its E_{EA} value (3.1 eV) is 0.6 eV higher than that reported for the poly(2,3-dioctylthieno[3,4-b]pyrazine) homo-polymer (≈ 2.5 eV). An E_{IP} value of 4.64 eV and E_{EA} value of 2.8 eV were found in the case of

BTTP-P [19].

In this paper we are going to use a set of model parameters close to those encountered in polypeptide macromolecules or bridge-mediated donor-acceptor systems, summarized above. In particular, the following parameter values will be taken (see also [12]) for the α -helix parameters:

$$\mathcal{E}_0 = 0, \quad J = 0.145, \quad L = 0.231, \quad W = 1.825, \quad \chi = 0.318. \quad (12)$$

Before studying the transfer of an electron from the donor to the acceptor we have computed the profile of the static polaron on the helix for the parameters given in (12). This profile is shown on figure 2. To obtain this profile, we have relaxed the equations (11), using donor-acceptor parameter values so that they do not interact with the chain.

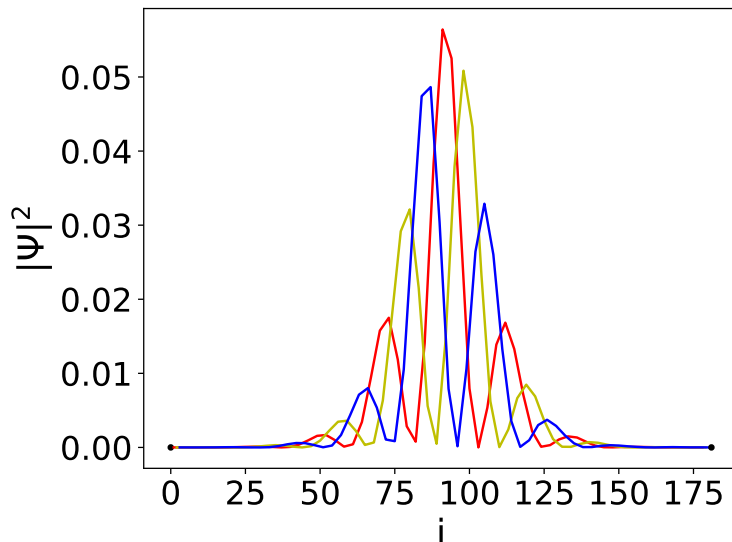


Figure 2: Polaron with $\mathcal{E}_0 = \mathcal{E}_d = \mathcal{E}_a = 0$, $J = 0.145$, $L = D_{d,3} = D_{a,1} = 0.231$, $D_{d,1} = D_{d,2} = D_{a,2} = D_{a,3} = 0$, $W = W_{d,1} = W_{d,2} = W_{d,3} = W_{a,3} = 1.825$, $W_{a,1} = W_{a,2} = 0$, $\chi_{d,\ell} = 0.318$, $\chi_{d,\ell} = \chi_{a,\ell} = 0$, $A_{a,ell} = 0$, $K_d = K_a = 1$. The electron probability density are plotted versus the index on the polypeptide chain. The 3 strands profiles are shown in different colours.

One sees clearly from figure 2, where the index i runs along the polypeptide helix and where each curve corresponds to a different strand, that the static polaron is a large partially delocalised lump which winds around the polypeptide chain rather than a single soliton located on a single strand or three identical solitons located on each of the strands. We also see that the

polaron is spread slightly in the direction transverse to the helix or, in other words, that its width is small but nevertheless larger than that of a single chain.

4 Classes of Couplings

Having so far defined a model with a general set of couplings between the α -helix and the donor and acceptor, we will now restrict ourselves to 3 families of couplings.

In the first set, the donor and the acceptor are coupled to all 3 strands of the helix using identical coupling parameters. So we have

$$\begin{aligned} D_{d,1} = D_{d,2} = D_{d,3}, & & D_{a,1} = D_{a,2} = D_{a,3}, \\ W_{d,1} = W_{d,2} = W_{d,3}, & & W_{a,1} = W_{a,2} = W_{a,3}. \end{aligned} \quad (13)$$

We call such a configuration the ‘full homogeneous’ coupling.

The second configuration describes the case in which the donor and the acceptor are coupled to only one strand, so that

$$\begin{aligned} D_{d,2} = D_{d,3} = 0, & & D_{a,2} = D_{a,3} = 0, \\ W_{d,2} = W_{d,3} = 0, & & W_{a,2} = W_{a,3} = 0, \\ A_{a,2} = A_{a,3} = 0. & & \end{aligned} \quad (14)$$

We call this the ‘single strand’ coupling. Notice that the donor is coupled to the first peptide of the helix, but the acceptor is coupled to the second but last peptide of the helix.

For the third configuration we consider the case when the donor and the acceptor are coupled only to the first and last peptides on the alpha-helix so

$$\begin{aligned} D_{d,2} = D_{d,3} = 0, & & D_{a,1} = D_{a,2} = 0, \\ W_{d,2} = W_{d,3} = 0, & & W_{a,1} = W_{a,2} = 0, \\ A_{a,1} = A_{a,2} = 0. & & \end{aligned} \quad (15)$$

We call this case the ‘end to end’ coupling.

To find the best parameter values for the transfer of the electron from the donor to the acceptor, we have integrated the system of equations (11) numerically on a lattice of 180 peptides. As the initial condition we have taken the case when the electron probability density was set to 1 on the donor and to 0 everywhere else. We then integrated the equations (11) numerically up to $\tau = 500$. This time was so chosen because it is roughly 3 times longer than it takes for the polaron to reach the end of the 180-peptides

chain. The value of $|\Psi_{N+1}|^2$ varies with time, but tends to increase modulo some fluctuations. To evaluate $\max |\Psi_{N+1}|^2$ we have tracked its value during the evolution and recorded the largest value obtained before $\tau \leq 500$.

We have first determined the best donor parameters so that the electron is fully transferred onto the α -helix. We then scanned a very large range of parameter values for the acceptor to determine the one for which the maximum value of the electron probability density on the acceptor, $\max |\Psi_{N+1}|^2$, reaches the largest value.

We will now describe the results we have obtained for each type of coupling.

4.1 Full Homogeneous Coupling

The best parameter values we have found to generate a transfer of electron from the donor to the acceptor are (assuming all the values of $A_{a,\ell}$, $D_{d,\ell}$, $D_{a,\ell}$, $W_{d,\ell}$, $W_{a,\ell}$, $\chi_{d,\ell}$ and $\chi_{a,\ell}$ are the same for $\ell = 1, 2, 3$):

$$\begin{aligned} \mathcal{E}_d = 0.25, \quad D_{d,\ell} = 0.38 J, \quad W_{d,\ell} = 0.32 W, \quad \chi_{d,\ell} = 0.62 \chi, \\ A_{a,\ell} = 0.62, \quad \mathcal{E}_a = 0.194, \quad D_{a,\ell} = 0.175 J, \quad W_{a,\ell} = 0.14 W, \quad \chi_{a,\ell} = 0.27 \chi, \end{aligned} \quad (16)$$

and we have found that $\max |\Psi|^2 = 0.896$ for $\tau \leq 500$.

In figure 3 we present the plots of the time-evolution of the probability density of the electron for the parameters values (12) and (16). We see clearly that the electron is transferred from the donor onto the chain and that it then forms a wave that propagates on the chain (see the movie in the supplementary material). There are at least two polarons of different profiles which propagate on the α -helix polypeptide chain, rather than on the strands. The polarons are followed by what looks like incoherent ripples which also propagate on the α -helix.

We have then studied how $\max |\Psi_{N+1}|^2$ varies when the acceptor parameters are varied around their optimal value. This is shown in figures 4-9.

To perform these simulations, we have defined the following parameters

$$D_a S = \frac{D_{a,\ell}}{J}, \quad W_a S = \frac{W_{a,\ell}}{W}, \quad X_a S = \frac{\chi_{a,\ell}}{\chi}, \quad (17)$$

which relate the different parameters of the donor and the acceptor to the corresponding ones on the peptide chain.

From figures 4 and 5, we first note that the value of the acceptor electron energy E_a has to be relatively small for the electron to be transferred to the acceptor, and that the values of \mathcal{E}_a and A_a must be finely tuned for a good absorption. The parameters D_a and W_a and χ_a , on the other hand, offer a

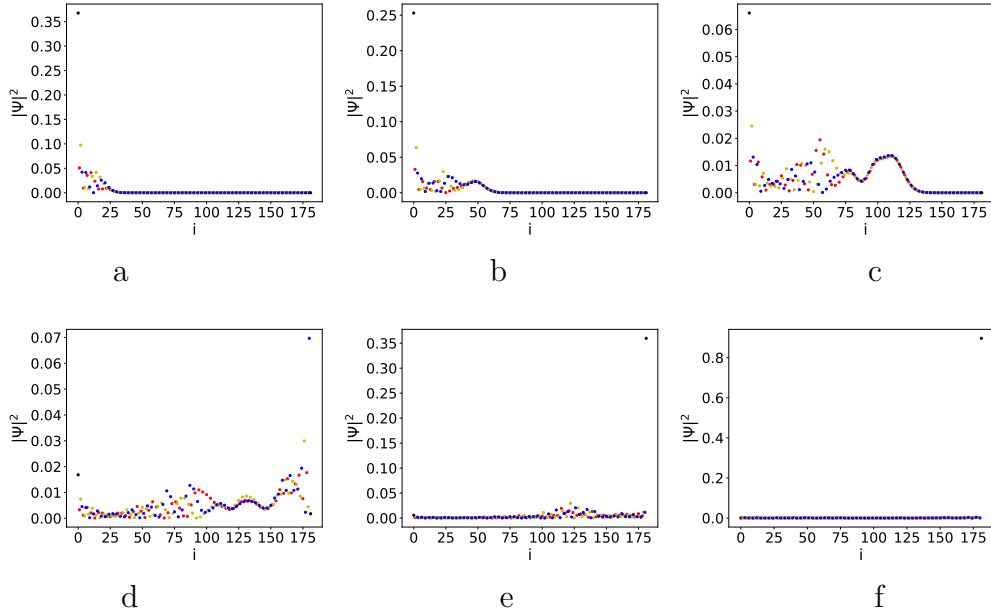


Figure 3: Profile of $|\Psi|^2$ for the full homogeneous coupling during the transfer from donor to acceptor. a) $\tau = 25$, b) $\tau = 50$, c) $\tau = 100$, d) $\tau = 150$, e) $\tau = 200$, f) $\tau = 500$.

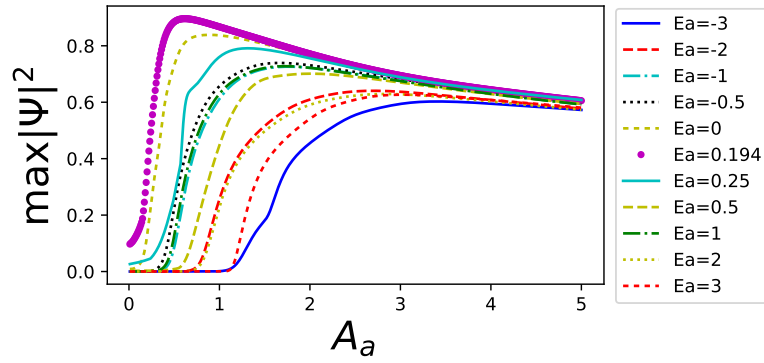


Figure 4: Full homogeneous coupling. The plot of $\max(|\Psi_{N+1}|^2)$ for $\tau \leq 500$ as a function of A_a for different values of \mathcal{E}_a and the parameters values (16).

much broader tolerance when \mathcal{E}_a and A_a are correctly tuned (see figures 6 to 9).

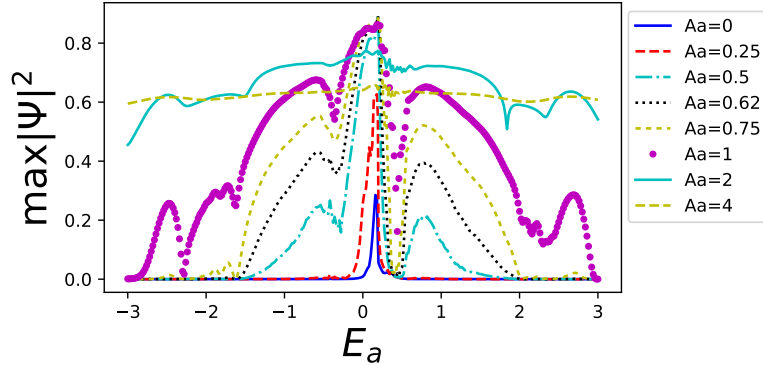


Figure 5: Full homogeneous coupling. The plot of $\max(|\Psi_{N+1}|^2)$ for $\tau \leq 500$ as a function of E_a for different values of $A_{a,1} = A_{a,2} = A_{a,3} = A_a$ and the parameters values (16).

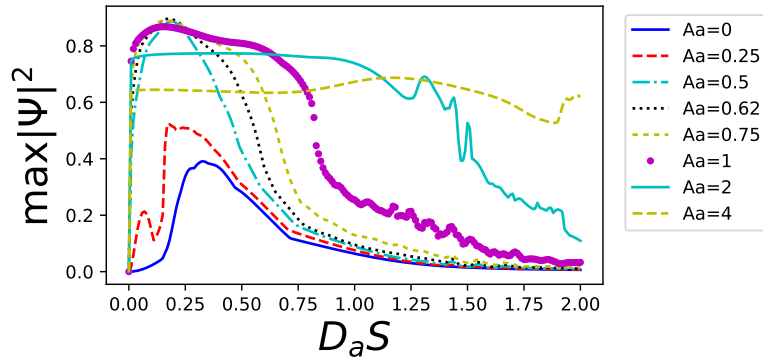


Figure 6: Full homogeneous coupling. The plot of $\max(|\Psi_{N+1}|^2)$ for $\tau \leq 500$ as a function of $D_a S = D_{a,\ell}/J$ for different values of $A_{a,1} = A_{a,2} = A_{a,3} = A_a$ and the parameters values (16).

4.2 Single Coupling

In this section we couple the donor only to the first node of the chain: $D_{d,2} = D_{d,3} = W_{d,2} = W_{d,3} = \chi_{d,2} = \chi_{d,3} = 0$. We obtain the best transfer from the donor to the chain for the following donor parameters:

$$\mathcal{E}_d = 0.25, \quad D_{d,1} = 0.38 J, \quad W_{d,1} = 0.32 W, \quad \chi_{d,1} = 0.62 \chi. \quad (18)$$

We then coupled the acceptor to only one peptide on the chain in two different ways: first, to the same strand as the one to which the donor is coupled (single-strand coupling) and then to the last peptide on the chain (end-to-end coupling).

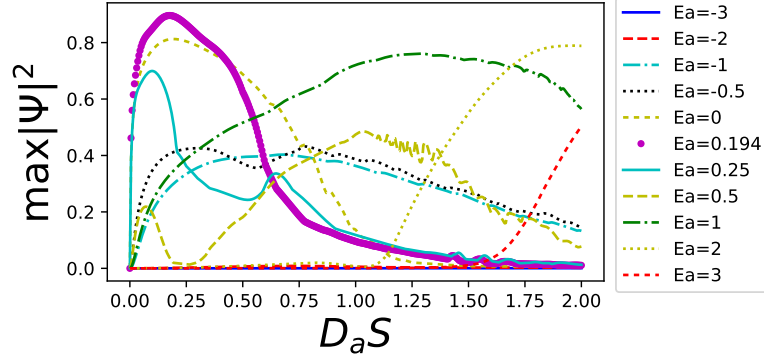


Figure 7: Full homogeneous coupling. The plot of $\max(|\Psi_{N+1}|^2)$ for $\tau \leq 500$ as a function of $D_a S = D_{a,\ell}/J$ for different values of \mathcal{E}_a and the parameters values (16).

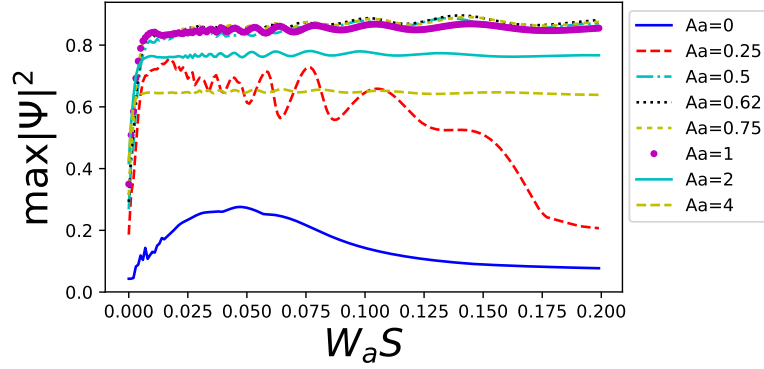


Figure 8: Full homogeneous coupling. The plot of $\max(|\Psi_{N+1}|^2)$ for $\tau \leq 500$ as a function of $W_a S = W_{a,\ell}/W$ for different values of $A_{a,1} = A_{a,2} = A_{a,3} = A_a$ and the parameters values (16).

4.2.1 Single-Strand Coupling

To couple the acceptor to the same strand as the donor, we take $A_{a,2} = A_{a,3} = D_{a,2} = D_{a,3} = W_{a,2} = W_{a,3} = \chi_{a,2} = \chi_{a,3} = 0$.

We then found that the best parameters to obtain a transfer of the electron to the acceptor are

$$\begin{aligned} \mathcal{E}_d = 0.25, \quad D_{d,1} = 0.38 J, \quad W_{d,1} = 0.32 W, \quad \chi_{d,1} = 0.62 \chi, \\ A_{a,1} = 6.5, \quad \mathcal{E}_a = 0.265, \quad D_{a,1} = 0.3 J, \quad W_{a,1} = 0.37 W, \quad \chi_{a,1} = \chi. \end{aligned} \quad (19)$$

Unfortunately the maximum value of $|\Psi_{N+1}|^2$ for $\tau \leq 500$ was only 0.21839, showing that in this configuration, the electron is only transferred to the

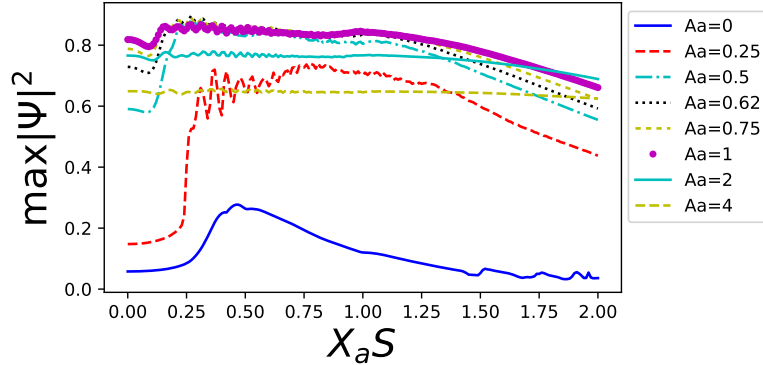


Figure 9: Full homogeneous coupling. The plot of $\max(|\Psi|^2)$ for $\tau \leq 500$ as a function of $\chi_a S = \chi_{a,\ell}/\chi$ for different values of $A_{a,1} = A_{a,2} = A_{a,3} = A_a$ and the parameters values (16).

acceptor with a 20% probability. As this is quite small we did not study the variation of $\max |\Psi_{N+1}|^2$ around these optimal values of the parameters.

4.2.2 End-to-End Coupling

To couple the acceptor to the last peptide of the helix, we must take $A_{a,1} = A_{a,2} = D_{a,1} = D_{a,2} = W_{a,1} = W_{a,2} = \chi_{a,1} = \chi_{a,2} = 0$. In this case we have obtained the best transfer using the following parameters:

$$\begin{aligned} \mathcal{E}_d = 0.25, \quad D_{d,1} = 0.38 J, \quad W_{d,1} = 0.32 W, \quad \chi_{d,1} = 0.62 \chi, \\ A_{a,3} = 1.98, \quad \mathcal{E}_a = 0.276, \quad D_{a,3} = 0.29 J, \quad W_{a,3} = 0.002 W, \quad \chi_{a,3} = 0.04 \chi, \end{aligned} \quad (20)$$

and, with this choice, we have found that $\max |\phi_{N+1}|^2 = 0.642558$, We have then studied how $\max |\Psi_{N+1}|^2$ varies when the acceptor parameters are varied around their optimal value. This is shown in figures 10 to 15.

As with the full homogeneous coupling, we have found that the absorption is mainly controlled by a fine tuning between $A_{a,3}$ and E_a but that there is a broader tolerance for the values of D_a , W_a and χ_a .

Having analysed the parameter stability of our model we now turn to the study of its thermal stability.

5 Thermal Stability of the Soliton-Mediated Electron Transport

So far, in the study of our model, we have not taken into account any thermal fluctuations. To include them we have modified the model by adding the

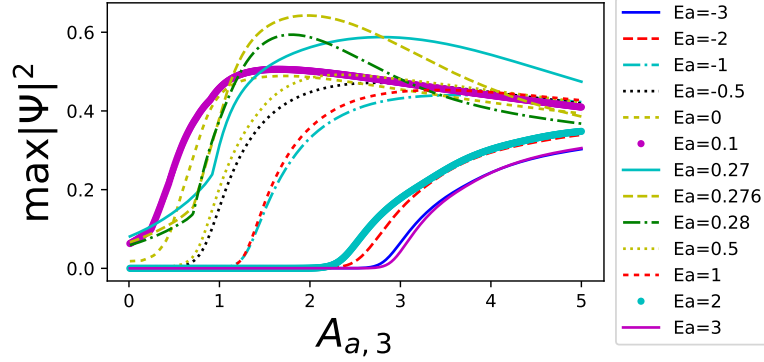


Figure 10: End-to-end coupling. The plot of $\max |\Psi_{N+1}|^2$ for $\tau \leq 500$ as a function of $A_{a,3}$ for different values of \mathcal{E}_a and the parameters values (21).

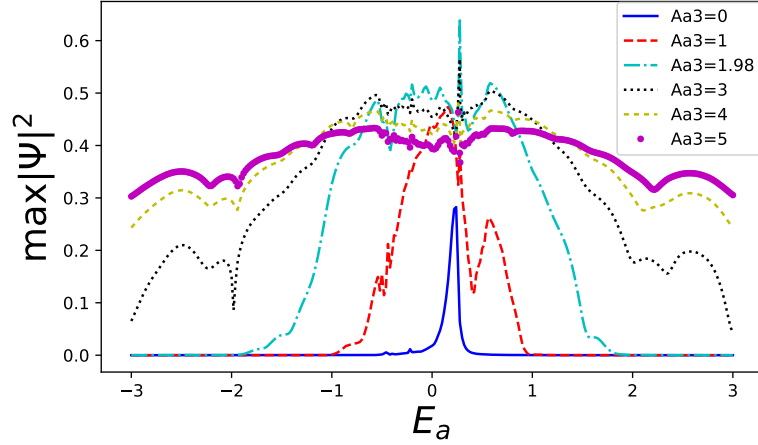


Figure 11: End-to-end coupling. The plot of $\max |\Psi_{N+1}|^2$ for $\tau \leq 500$ as a function of E_a for different values of $A_{a,3}$ and the parameters values (21).

following Langevin term to the equations for U_n :

$$L_n = F_n(\tau) - \Gamma \frac{du_n}{d\tau}, \quad (21)$$

where Γ is an absorption parameter and $F_n(\tau)$ represents the thermal noise as a Gaussian white noise of zero mean value and variance given by

$$\langle F_n(\tau_1) F_m(\tau_2) \rangle = 2\Gamma kT \delta(\tau_1 - \tau_2) \delta_{n,m}, \quad (22)$$

where, for the dimensional thermal energy \overline{kT} , we have $kT = \overline{kT}/\overline{J}$. To implement this numerically, $F(\tau)$ has to be kept constant during each time step $d\tau$ and so we have used $\delta(\tau_1 - \tau_2) = 1/d\tau$.

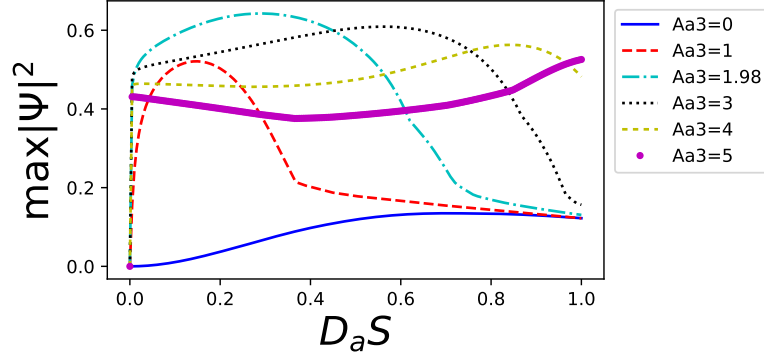


Figure 12: End-to-end coupling. The plot of $\max |\Psi_{N+1}|^2$ for $\tau \leq 500$ as a function of $D_a S = D_{a,\ell}/J$ for different values of $A_{a,3}$ and the parameters values (21).

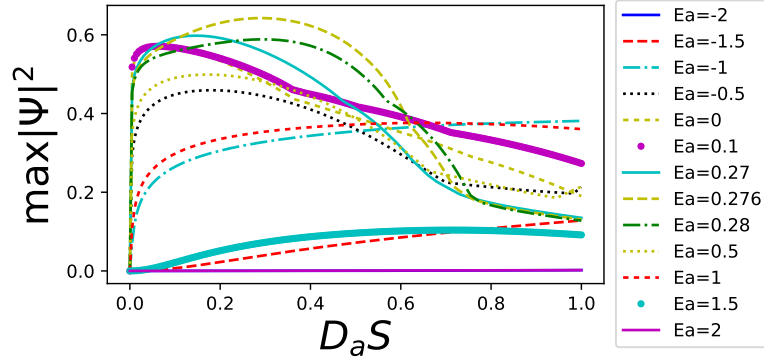


Figure 13: End-to-end coupling. The plot of $\max |\Psi_{N+1}|^2$ for $\tau \leq 500$ as a function of $D_a S = D_{a,\ell}/J$ for different values of \mathcal{E}_a and the parameters values (21).

For each temperature, we have performed 100 simulations and computed the mean values of $\max |\Psi_a|$, for $\tau \leq 500$, obtained from these simulations.

At physiological temperature, $\overline{kT} \approx 0.025eV$ while \overline{J} in α -helices is of the order of $0.1eV$. This means that in our dimensionless units, $kT \approx 0.25$. We have thus varied kT between 0 and 1 to capture the physiological conditions when \overline{J} is smaller than $0.1eV$.

In figure 16 we present the variation of $\max |\Psi_{N+1}|^2$ as a function of temperature for different chain lengths. We see that for short chains, the temperature has a minimal effect while for longer chains, its influence is more pronounced. In trans-membrane proteins, the α -helices are relatively short with $N = 30$ or even smaller. This means that under physiological conditions, the transfer of the electron from a donor to an acceptor is thermally stable.

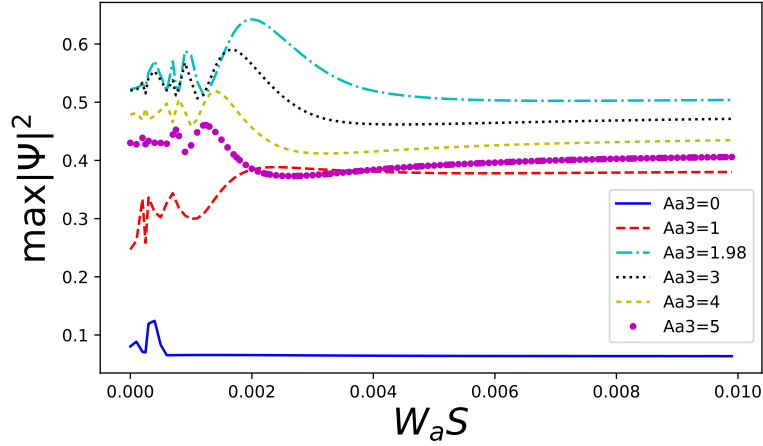


Figure 14: End-to-end coupling. The plot of $\max |\Psi_{N+1}|^2$ for $\tau \leq 500$ as a function of $W_a S = W_{a,\ell}/W$ for different values of $A_{a,3}$ and the parameters values (21).

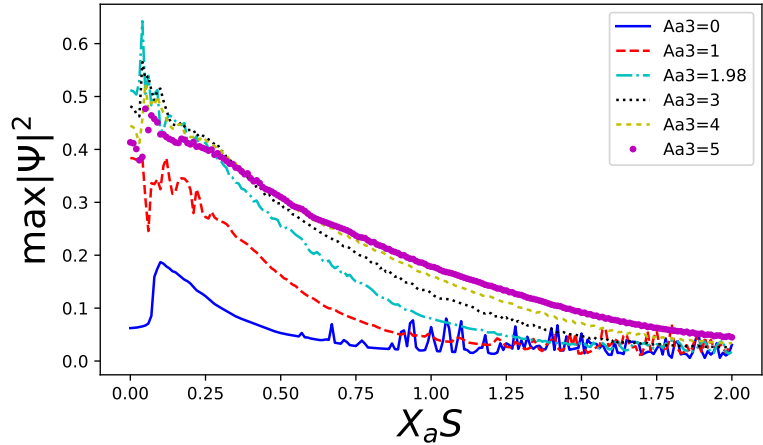


Figure 15: End-to-end coupling. The plot of $\max |\Psi_{N+1}|^2$ for $\tau \leq 500$ as a function of $\chi_a S = \chi_{a,\ell}/\chi$ for different values of $A_{a,3}$ and the parameters values (21).

Looking at the data in figure 17 we see that the probability of a transfer of the electron from the donor to the acceptor decreases as the friction parameter, Γ , increases. For shorter chains, the effect is very small, but for very long ones, the effect is more pronounced. As the α -helices found in transmembrane proteins are relatively short, one can conclude that the value of Γ , which can only be estimated, does not play a significant role on the thermal stability of the electron transfer.

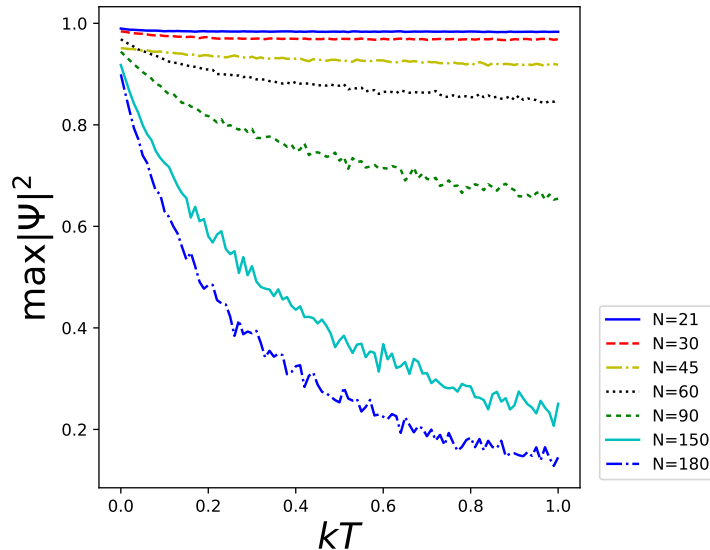


Figure 16: Full homogeneous coupling. The plot of $\max |\Psi_{N+1}|^2$ for $\tau \leq 500$ as a function of kT for different values of the chain length N . $\Gamma = 0.2$.

6 Conclusions

In this paper we have presented a model describing the long-range transport of an electron from a donor molecule to an acceptor one via the polaron state formed in a α -helical protein in a ‘Donor – α -helix – Acceptor’ system. The α -helix was modelled as a polypeptide chain in which each peptide was coupled to its nearest neighbours by a chemical bond and to every 3rd neighbour by a hydrogen bond. The helix could then also be described as 3 parallel strands coupled to each other. We have found that the static polaron on such a chain, for the parameters that best describe an α -helical protein, is a partially delocalised hump along the polypeptide backbone rather than being located on the individual strands. This confirms that the traditional approximation of assuming that the polaron is equally distributed on the 3 strands is not bad for broad polarons (see also [10, 12]).

We have then studied the transfer of an electron from a donor molecule to the acceptor by initially placing the electron on the donor. For the proper parameters of the couplings, the electron was, within very short time interval, transferred onto the polypeptide chain where it was self-trapped in a polaron state, and then moved towards the other extremity of the chain where it was absorbed by the acceptor.

We have considered three types of couplings between the donor and the polypeptide chain as well as between the acceptor and the polypeptide chain.

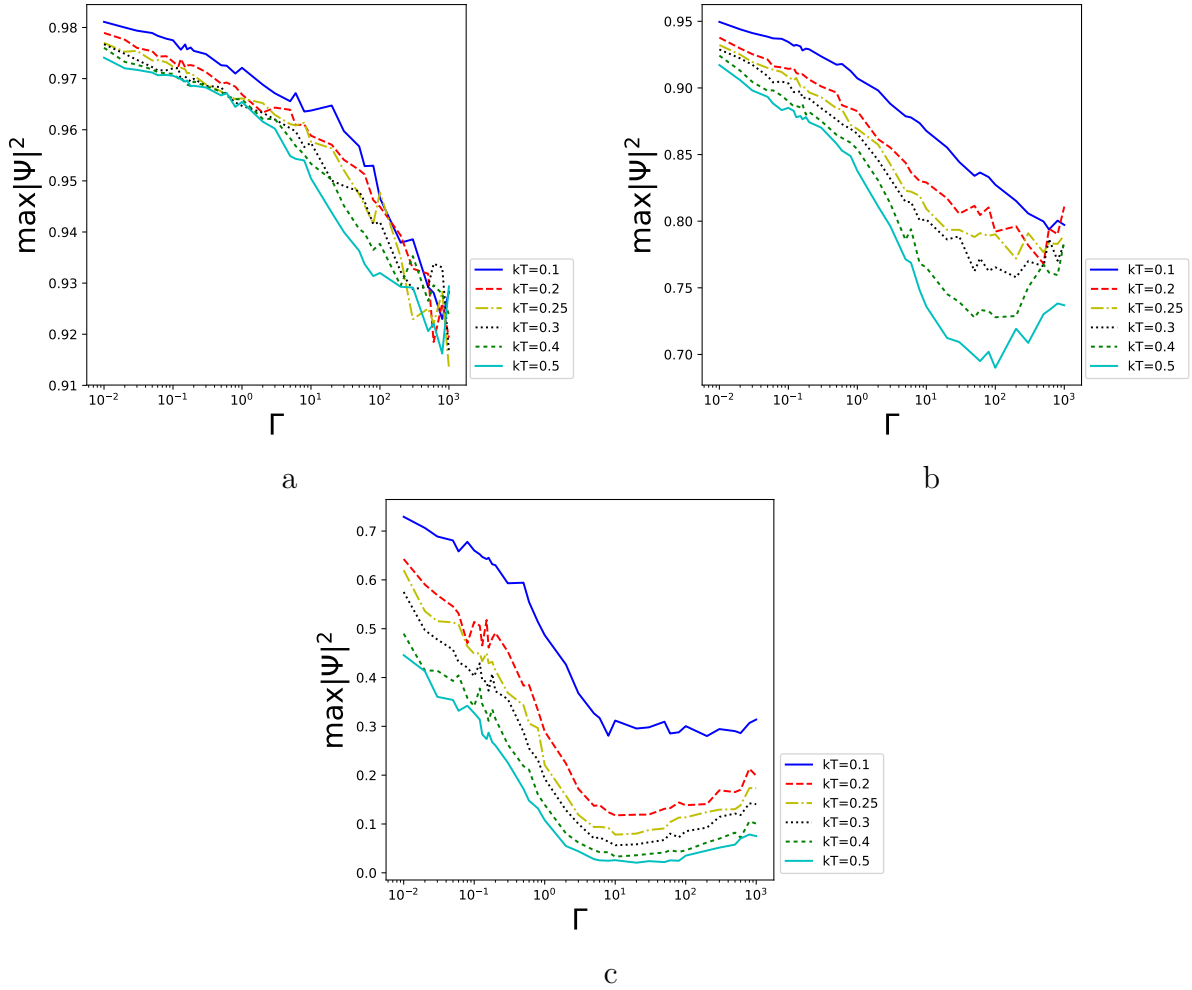


Figure 17: Full homogeneous coupling. The plot of $\max |\Psi_{N+1}|^2$ for $\tau \leq 500$ as a function of Γ for different values of kT . a) $N = 30$, b) $N = 60$, c) $N = 180$.

In the first case, the donor and the acceptor were coupled, respectively, to the first 3 and the last 3 nodes of the chain, using the identical parameters and we called such a configuration the ‘fully homogeneous’ one. In the second configuration, the donor was coupled to the first node of the chain and the acceptor to the last node of the same strand, or in other words to the 3rd node from the end. We called such a coupling ‘single-strand’ one. For the last configuration, the donor was coupled to the first node of the chain and the acceptor to the last node of the chain and we called this ‘end-to-end’ coupling.

The fully homogeneous coupling is the one that leads to the best donor-

acceptor electron transport with the efficiency of 90% or more depending on the length of the chain. The ‘end-to-end’ coupling did not work so well and led to a transfer probability of only 60% while the ‘single-strand’ one was the worst leading only to a 20% probability transfer.

Our study has shown that an electron in the polaron (soliton-like) state can easily propagate as a travelling wave along the α -helical chain. The polaron that is generated at the terminal of the helix in the vicinity of the donor molecule has a complex internal structure: it is not just a clean simple polaron but can be described as a non-linear superposition of at least 2 polarons of different sizes which propagate on the α -helical backbone rather than on the individual strands; this indicates the collective ‘hybrid’ nature of the polaron.

We have also shown that when we add thermal fluctuations to the model, the long range electron transfer in the ‘Donor – α -helix – Acceptor’ system is stable at physiological temperatures.

7 Acknowledgement

One of us, LSB, acknowledges the partial support from the budget program KPKVK 6541230 and the scientific program 0117U00236 of the Department of Physics and Astronomy of the National Academy of Sciences of Ukraine and thanks the Department of Mathematical Sciences of the University of Durham for the hospitality during her short-term visit.

References

- [1] J. Jortner, M. Bixon, editors *Electron Transfer From Isolated Molecules to Biomolecules*. Adv. Chem. Phys., **106**. John Wiley and Sons, Inc., New York, NY, 1999
- [2] Voet D, Voet JG . *Biochemistry* (3rd ed.). John Wiley and Sons. 2004. ISBN 978-0-471-58651-7.
- [3] Frster, Theodor (1948). "Zwischenmolekulare Energiewanderung und Fluoreszenz" [Intermolecular energy migration and fluorescence]. *Annalen der Physik* (in German). 437 (12): 5575. Bibcode:1948AnP...437...55F. doi:10.1002/andp.19484370105
- [4] M. Kasha. Energy transfer, charge transfer, and proton transfer in molecular composite systems. In: M. Kasha ed., *Physical and Chem-*

- ical Mechanisms in Molecular Radiation Biology*. Springer, p 231-255. 1992.
- [5] Jones, Garth A; Bradshaw, David S (2019). *Frontiers in Physics*. 7: 100.doi:10.3389/fphy.2019.00100
- [6] Murray, Robert K.; Daryl K. Granner; Peter A. Mayes; Victor W. Rodwell (2003). *Harper's Illustrated Biochemistry*. New York, NY: Lange Medical Books/ McGraw Hill. p. 96. ISBN 0-07-121766-5.
- [7] Davydov, A.S. and Kislukha, N.I. (1973) *Physica Status Solidi (b)*, 59, 465-470. <https://doi.org/10.1002/pssb.2220590212>
- [8] A.S. Davydov, *Solitons in Molecular Systems* (Dordrecht, Reidel, 1985).
- [9] A.C.Scott. *Phys. Rep.*, **217** 1, 1992.
- [10] A. S. Davydov, A. A. Eremko, and A. I. Sergienko, *Ukr. J. Phys.* 23, 983 (1978)
- [11] V. K. Fedyanin and L. V. Yakushevich, *Int. J. Quantum Chem.* 21, 1019 (1982).
- [12] L.S. Brizhik, A.A. Eremko, B. Piette W.J. Zakrzewski. *Phys. Rev. E* 70, 031914, p.1-16 (2004).
- [13] L.S. Brizhik, A.A. Eremko, *Z. Phys. B*, 1997, 104, 771-775.
- [14] L. Brizhik, B. Piette, W. Zakrzewski. *Phys.Rev. E* 90 (2014) 052915 DOI: <http://dx.doi.org/10.1103/PhysRevE.90.052915>
- [15] L.S. Brizhik, A.S. Davydov, *Phys. Stat. Sol. (b)*, **115** 615-630 (1983)
- [16] L.S. Brizhik. *Phys. Rev.B1*, **48** 3142-3144 (1993).
- [17] Nicholls DG; Ferguson SJ (July 2002). *Bioenergetics 3*. Academic Press. ISBN 978-0-12-518121-1.
- [18] James A. Roberts , James P. Kirby , Daniel G. Nocera *J. Am. Chem. Soc.*, , **117** (30), pp 80518052 (1995) DOI: 10.1021/ja00135a038
- [19] Y. Zhu , R. D. Champion , S.A. Jenekhe , *Macromolecules*, **39** (25), 87128719 (2006); DOI: 10.1021/ma061861g
- [20] Dan Li, Chen Sun, Hao Li, Hui Shi, et al *Chem. Sci.*, 2017, **8**, 4587-4594 , DOI:10.1039/C7SC00077D

- [21] Q. Van Nguyen, P. Martin, D. Frath, et al. *J. Am. Chem. Soc.* 2018, 1403210131-10134, Publication Date: July 30, 2018
- [22] Tian L, Hu Z, Liu X, et al, *ACS Appl Mater. Interfaces.* 2019 Feb 6; **11**(5) 5289-5297. doi: 10.1021/acsami.8b19036. Epub 2019 Jan 23.
- [23] H. Li, F.S. Kim, G. Ren, and S.A. Jenekhe, *J. Am. Chem. Soci.* 135 (40), 14920-14923 (2013)
- [24] H. A. M. van Mullekom, J. A. J. M. Vekemans, E. E. Havinga, and E. W. Meijer, *Mater. Sci. Eng.* 32, 1 (2001).
- [25] Y. Zhu, R. D. Champion, and S. A. Jenekhe, *Macromolecules*, 39, 8712 (2006).
- [26] G. Yu, J. Gao, J. C. Hummelen, F. Wudl, and A. J. Heeger, *Science* 270, 1789 (1995).
- [27] L.M. Campos, A. Tontcheva, S. Günes, G. Sonmez, Neugebauer, N. S. Sariciftci, and F. Wudl, *Chem. Mater.* 17, 4031 (2005).
- [28] M. Svensson, F. Zhang, S. C. Veenstra, W. J. H. Verhees, C. Hummelen, J. M. Kroon, O. Inganäs, and M. R. Andersson, *Adv. Mater.* 15, 988 (2003).
- [29] , S. Admassie, O. Inganäs, W. Mammo, E. Perzon, and M. R. Andersson, *Synth. Met.* 156, 614 (2006).
- [30] A. P. Kulkarni, Y. Zhu, and S. A. Jenekhe, *Macromolecules* 38, 1553 (2005).
- [31] C. Ego, D. Marsitzky, S. Becker, J. Zhang, A. C. Grimsdale, Mullen, J. D. MacKenzie, C. Silva, and R. H. Friend, *J. Am. Chem. Soc.* 125, 437 (2003)
- [32] Thompson, B. C., Madrigal L. G., Pinto M. R., Kang T.-S., Schanze K. S., Reynolds J. R., *J. Polym. Sci., Part A: Polym. Chem.* 43, 1417 (2005).
- [33] Wu W.-C., Liu, C.-L., Chen, W.-C., *Polymer*, 47, 527 (2006).
- [34] Babel, J. D. Wind, and S. A. Jenekhe, *Adv. Funct. Mater.* 14, 891 (2004).
- [35] T. Yamamoto, T. Yasuda, Y. Sakai, and S. Aramaki, *Macromol. Rapid Commun.* 26, 1214 (2005).

- [36] M. Chen, X. Crispin, E. Perzon, M. R. Andersson, T. Pullerits, M. Andersson, O. Inganäs, and M. Berggren, *Appl. Phys. Lett.* **87**, 252105 (2005).
- [37] T. Yasuda, Y. Sakai, S. Aramaki, and T. Yamamoto, *Chem. Mater.* **17**, 6060 (2005)
- [38] H. Zhang, S. Zhang, Y. Mao, et al. *Polym. Chem.*, 2017, **8**, 3255-3260, DOI:10.1039/C7PY00616K
- [39] A.S. Davydov and A.D. Suprun. *Ukr. J. Phys.* **19** 44, 1974.
- [40] A.S. Davydov, *J.Theor. Biol.* **38** 559, 1973.
- [41] Engel G S, Calhoun T R, Read E L, Ahn T K, Mancal T, Cheng Y C, Blankenship R E and Fleming G R 2007 *Nature* 446 782786
- [42] Collini E, Wong C Y, Wilk K E, Curmi P M G, Brumer P and Scholes G D 2010 *Nature* 463 644647
- [43] T. Renger , V. May , O. Kühn, *Phys. Rep.* **343** 137 (2001).
- [44] H. Wang ,S. Lin , J.P. Allen , J.C. Williams , S. Blankert, C. Laser, N.W. Woodbury, *Science* **316** 747 (2007).